ELSEVIER

Journal of Alloys and Compounds 356–357 (2003) 105–108

Journal of ALLOYS AND COMPOUNDS

www.elsevier.com/locate/jallcom

Structural investigation of hydrogen solubility in Y_yR_{1-y} alloys (R=Tb and Gd)

Y. Nakamura[a], P. Vajda[b,*], O.J. Zogal[c], E. Akiba[a]

[a] *National Institute of Advanced Industrial Science and Technology, Tsukuba, Ibaraki 305-8565, Japan*
[b] *Laboratoire des Solides Irradiés, Ecole Polytechnique, F-91128 Palaiseau, France*
[c] *Institute for Low-Temperature and Structure Research PAN, PL-50950 Wroclaw, Poland*

Received 1 June 2002; accepted 25 October 2002

Abstract

We have studied the structure of hydrogen loaded Y_yTb_{1-y} alloys, with $y=0.2$ and 0.9, by X-ray diffraction (XRD) techniques. The room-temperature XRD profiles of $Y_{0.2}Tb_{0.8}H_x$ exhibit, in addition to the peaks of the h.c.p. metal lattice, those of the f.c.c. dihydride for all $x>0$. In the case of $Y_{0.9}Tb_{0.1}H_x$, the f.c.c. peaks show up only for $x=0.20$, indicating H-solubility for smaller hydrogen concentrations in this alloy. As for the two Y_yGd_{1-y} ($y=0.3$ and 0.4) alloys, we observe in both cases precipitation of the dihydride for the smallest H concentrations. These results complement earlier resistivity measurements on the same systems, by presenting the evolution of the respective lattice parameters and their c/a ratios upon hydrogen addition and, in particular, specifying the influence of the metal lattice environment upon the state of the precipitating hydride.

Keywords: Hydrogen solubility; Y–Tb, Y–Gd Alloys; X-Ray diffraction

1. Introduction

We have recently started a series of investigations of (Y–R)H_x alloys [1–3] in order to advance in the understanding of the peculiar phenomenon of the low-temperature α*-RH_x solid solution phase, which represents a modulated quasi-unidimensional H–R–H pair structure along the *c*-axis and exists only in some of the rare earth metals (for a review, see e.g., Ref. [4]). It had been suggested [1,5]—based on an investigation of the modulated antiferromagnetism in rare earths and its c/a-dependence [6]—that the Fermi surface topology, in particular the critical dimensions of its webbing features, was responsible for the manifestation of both the spin-density waves (modulated AF) and the charge-density waves (modulated chains of H–R–H pairs). In our resistivity studies [1–3], we had confirmed this model for the systems Y_yTb_{1-y} and Y_yGd_{1-y}, showing that the presence of the α*-phase was restricted to the alloy $Y_{0.9}Tb_{0.1}H_x$ while, in the Tb-richer alloy (with $y=0.2$) and the two Y–Gd alloys, one observed precipitation of the dihydride (β-phase) for the smallest H concentrations.

It was interesting to complete these investigations by structural studies, in order to follow the evolution of the respective lattice parameters with *x* and, in particular to specify the type of dihydride precipitating in these alloys. In the X-ray diffraction study described in the following, we shall try to give the first answers to these questions.

2. Experimental

The specimens measured in these experiments were selected from the lot perused in the resistivity studies [1–3] where details of their preparation can be found. The hydrogen concentrations in each alloy system are given in Tables 1 and 2. The samples were cut into mm^2-sized pieces of roughly 200 μm thickness for X-ray diffraction investigation. The specimens were put on a holder with a 200-μm-deep edge. The holder is specially made by cutting silicon along planes which show no diffraction peak under the present diffraction conditions. The mea-

*Corresponding author. Tel.: +33-1-6933-4509; fax: +33-1-6933-3022.
E-mail address: peter.vajda@polytechnique.fr (P. Vajda).

0925-8388/02/$ – see front matter
doi:10.1016/S0925-8388(02)01219-7

Table 1
Lattice parameters of the observed phases in $Y_yTb_{1-y}H_x$

	x	a (Å)	c (Å)	c/a	$a(\beta)$ (Å)
$y=0.9$	0	3.6433(3)	5.7296(3)	1.5726	–
	0.05	3.6484(3)	5.7430(3)	1.5741	–
	0.15	3.6567(3)	5.7720(2)	1.5785	–
	0.20	3.6574(4)	5.7797(4)	1.5803	5.2122(6)
	0.25	3.6579(4)	5.7775(4)	1.5795	5.2100(5)
$y=0.2$	0	3.6132(2)	5.6993(2)	1.5774	–
	0.02	3.6140(3)	5.7031(3)	1.5781	5.245(1)
	0.10	3.6140(2)	5.7030(3)	1.5780	5.240(1)
	0.10D	3.6147(3)	5.7031(3)	1.5778	5.2383(7)
	0.20	3.6159(3)	5.7037(4)	1.5774	5.245(1)

Table 2
Lattice parameters of the observed phases in $Y_yGd_{1-y}H_x$

	x	a (Å)	c (Å)	c/a	$a(\beta)$ (Å)
$y=0.4$	0	3.6437(4)	5.7586(4)	1.5804	–
	0.10	3.6430(3)	5.7675(3)	1.5832	5.268(2)
	0.20	3.6440(5)	5.7680(5)	1.5829	5.267(2)
	0.25	3.6445(4)	5.7669(4)	1.5824	5.271(2)
$y=0.3$	0	3.6424(4)	5.7643(4)	1.5826	–
	0.05	3.6388(5)	5.7657(5)	1.5845	5.274(2)
	0.10	3.6394(5)	5.7673(5)	1.5847	5.280(7)
	0.20	3.6405(4)	5.7669(3)	1.5841	5.2767(8)

surements were performed on a diffractometer Rigaku RINT-2500V at 50 kV and 200 mA. Data were collected both for specimens alone and together with a Si standard; the latter was used for correcting slight displacements between sample surface and holder. The data were analyzed by Rietveld refinement software, RIETAN-2000 [7], which enables one to refine lattice parameters of multiphases simultaneously. To obtain correct lattice constants, we used a displacement parameter determined for each specimen.

3. Results and discussion

3.1. $Y_yTb_{1-y}H_x$ system

Fig. 1 shows the diffraction profiles of the five $Y_{0.9}Tb_{0.1}H_x$ samples measured at room temperature. On the fit (indicated by ticks below), we have separated the metallic lines (corresponding to the h.c.p. α*-solid solution) from the f.c.c. dihydride lines. The latter clearly emerge at $x=0.20$, indicating beginning precipitation from this concentration on. (The relative intensities of the lines are not significant, in view of the variously textured sample states). The alloy $Y_{0.2}Tb_{0.8}H_x$, however, exhibits (Fig. 2) the dihydride lines already for the smallest x-value measured ($x=0.02$), confirming the electrical resistivity data [1].

We have presented the lattice parameters of the various observed phases, after correction as described in Section 2, in Table 1 for comparison. The α*-phase parameters increase, for $y=0.9$, with x up to the maximum solubility at $x\approx0.2$ and remain constant above; the same is true for the c/a ratio, which we have plotted in Fig. 3, together

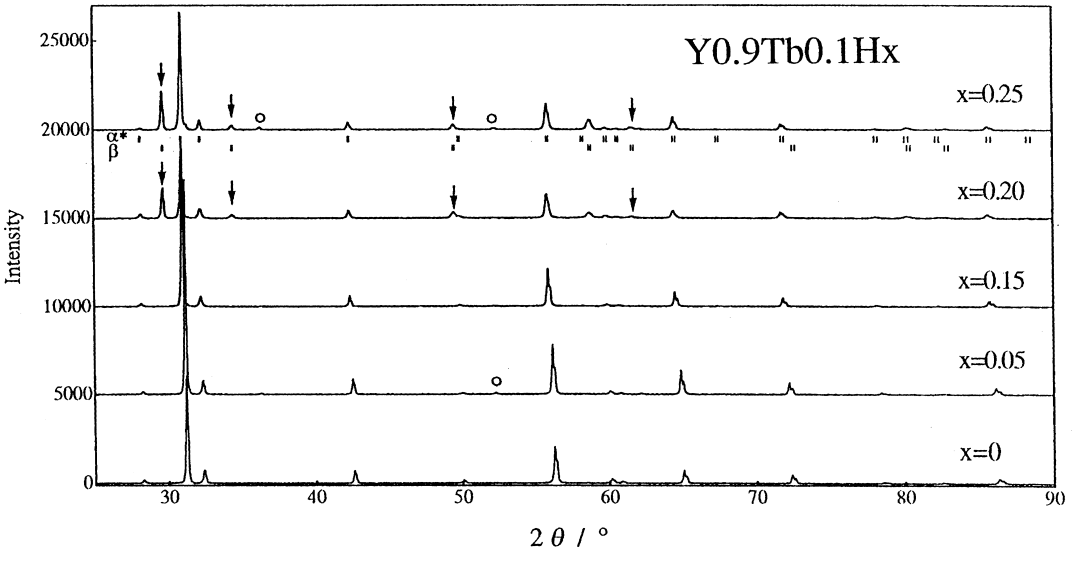

Fig. 1. X-Ray diffraction profiles of the $Y_{0.9}Tb_{0.1}H_x$ system, for various H concentrations, x. The ticks underneath correspond to positions of the diffraction lines for the h.c.p. α*-solid solution and of the f.c.c. β-RH_2 dihydride phases obtained from profile analysis. The lines due to the precipitating dihydride are indicated by arrows, impurity lines by open circles.

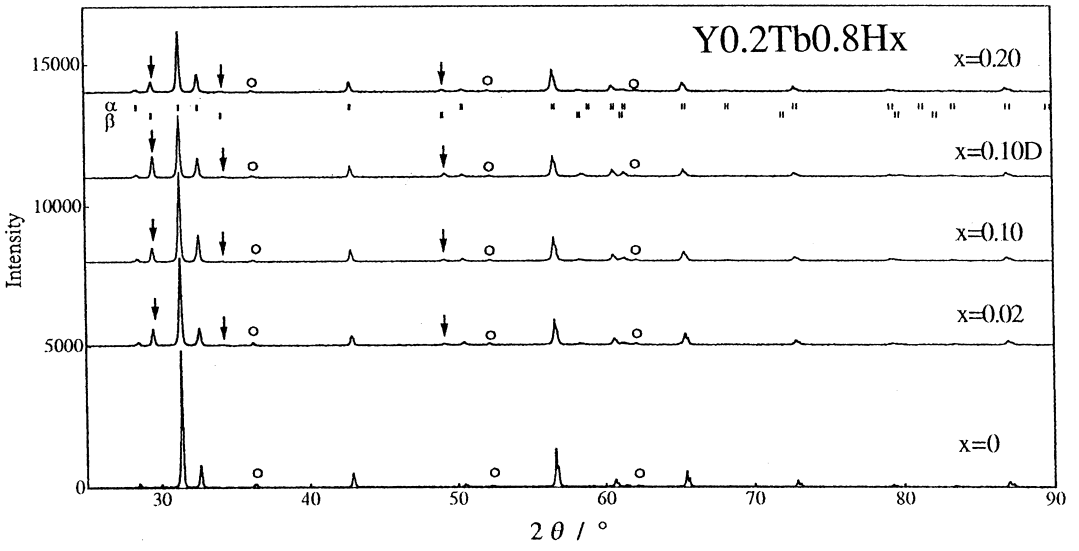

Fig. 2. Same as in Fig. 1, for the $Y_{0.2}Tb_{0.8}H_x$ system.

with the (roughly constant) c/a ratio of the $y=0.2$ alloy system. The H concentration dependence of resistivity $\rho(x)$ in the $y=0.9$ alloy, given in the inset and taken from Ref. [1], shows a nice parallelism in the electronic and structural properties.

It was interesting to determine the lattice parameter of the dihydride phase, since the ρ measurements [1] had clearly shown the precipitation of a magnetically ordering phase (at ≈10 K), hence obviously originating from the magnetic Tb component. A comparison with the $a(\beta)$ value of the pure dihydrides [4], $a(YH_2)=5.2082$ Å and $a(TbH_2)=5.2485$ Å, indicates, however, that the precipitating β-phase, despite its obvious TbH_2 character, takes the value of the structural majority component (in a kind of epitaxy), i.e. close to YH_2 for $y=0.9$ and to TbH_2 for $y=0.2$.

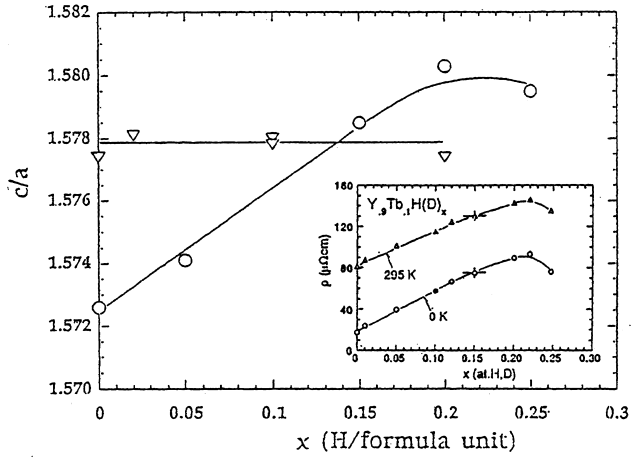

Fig. 3. c/a ratios as a function of the H concentration, for both $Y_yTb_{1-y}H_x$ systems, showing H solubility for $y=0.9$ (open circles) and immediate dihydride precipitation for $y=0.2$ (triangles). The $\rho(x)$-dependence of the $y=0.9$ system (inset) is taken from Ref. [1].

3.2. $Y_yGd_{1-y}H_x$ system

The profiles exhibited in Figs. 4 and 5 for the alloy systems $Y_{0.4}Gd_{0.6}H_x$ and $Y_{0.3}Gd_{0.7}H_x$, respectively, resemble those in Fig. 2 qualitatively, in the sense that the dihydride lines appear for the smallest H concentrations. (It is worth noting here the 'cleaner' profiles of the H-free alloys indicating the probable introduction of impurities during the loading procedure at high temperatures: contrary to the Y–Tb specimens, our pure Y–Gd samples had deliberately not been annealed, which is also the reason for their larger line widths).

Table 2 collects the corrected lattice parameters and the respective c/a ratios for all specimens, indicating their essentially x-independent behaviour. Again, as for Y–Tb (Table 1), the lattice constant $a(\beta)$ of the precipitating dihydride—though certainly corresponding to the magnetically ordering GdH_2 (see Refs. [2,3])—takes values between that of pure YH_2 and of GdH_2, $a(GdH_2)=5.3025$ Å [4], reflecting the decisive role of the environment.

In conclusion, the X-ray diffraction study of the investigated $(Y–Tb)H_x$ and $(Y–Gd)H_x$ alloy systems confirms the limited solubility of hydrogen in $Y_{0.9}Tb_{0.1}$ and the β-phase precipitation in all the others. Though certainly due to their magnetic (Tb or Gd) component, the values of $a(RH_2)$ are determined by the surrounding alloy environment rather than by those of the pure metals.

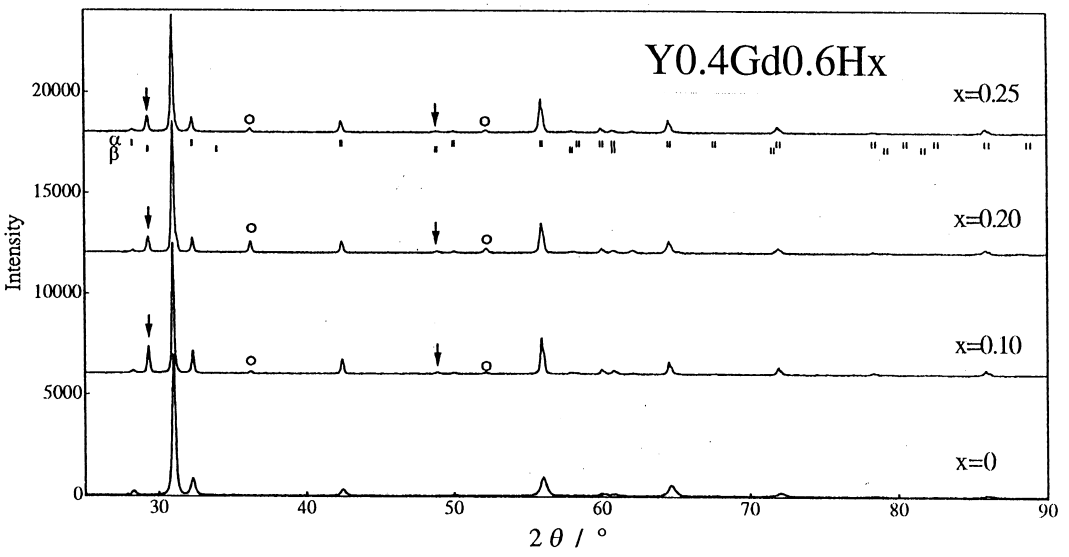

Fig. 4. Same as in Fig. 1, for the $Y_{0.4}Gd_{0.6}H_x$ system. Note the 'cleaner' spectrum (and the broader lines) in the non-annealed H-free alloy.

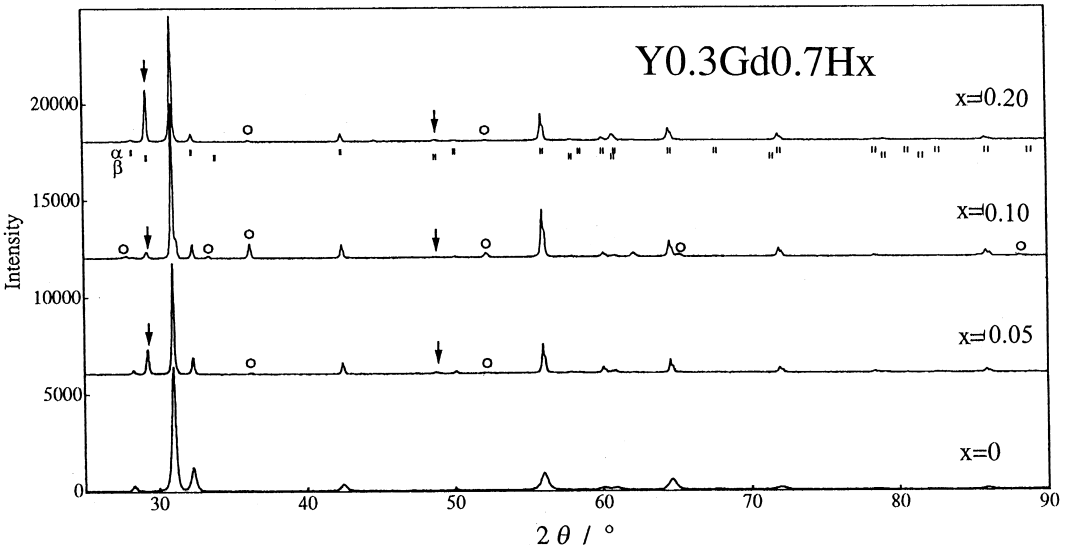

Fig. 5. Same as in Fig. 4, for the $Y_{0.3}Gd_{0.7}H_x$ system.

References

[1] P. Vajda, O.J. Zogal, Phys. Rev. B 59 (1999) 9467.
[2] P. Vajda, O.J. Zogal, Phys. Rev. B 61 (2000) 11232.
[3] P. Vajda, O.J. Zogal, J. Alloys Comp. 330–332 (2002) 381.
[4] P. Vajda, Hydrogen in rare earth metals, including RH_{2+x} phases, in: K.A. Gschneidner (Ed.), Handbook on the Physics and Chemistry of Rare Earths, Vol. 20, North Holland, 1995, p. 207.
[5] P. Vajda, Physica B 289/290 (2000) 435.
[6] A.V. Andrianov, J. Magn. Magn. Mater. 140/144 (1995) 749.
[7] F. Izumi, T. Ikeda, Mater. Sci. Forum 321/324 (2000) 198.